Electronic Supplementary Information

Large Au@Pd/PdO_x core-porous shell nanoparticles as efficient ethanol oxidation electrocatalysts

Junfang Hao,[a] Bin Liu,[a] Mari Takahashi,[b] Shinya Maenosono*[b] and Jianhui Yang*[a]

[a] Key Laboratory of Synthetic and Natural Functional Molecule Chemistry of Ministry of Education, Shaanxi Key Laboratory of Physico-Inorganic Chemistry, College of Chemistry & Materials Science, Northwest University, Xi'an 710069, P. R. China.

[b] School of Materials Science, Japan Advanced Institute of Science and Technology, 1-1 Asahidai, Nomi, Ishikawa 923-1292, Japan.

Corresponding Authors:

*E-mail: shinya@jaist.ac.jp

*E-mail: jianhui@nwu.edu.cn

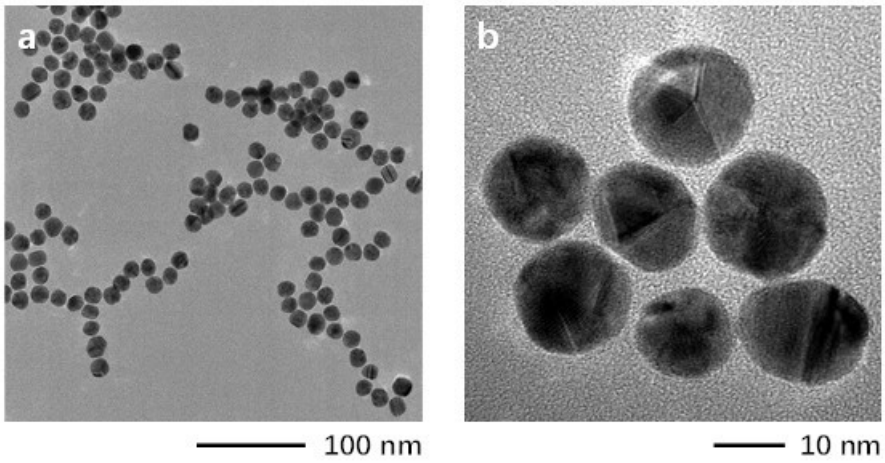

Fig. S1. (a) TEM and (b) HR-TEM images of Au seeds synthesized by the citrate-reduction method.

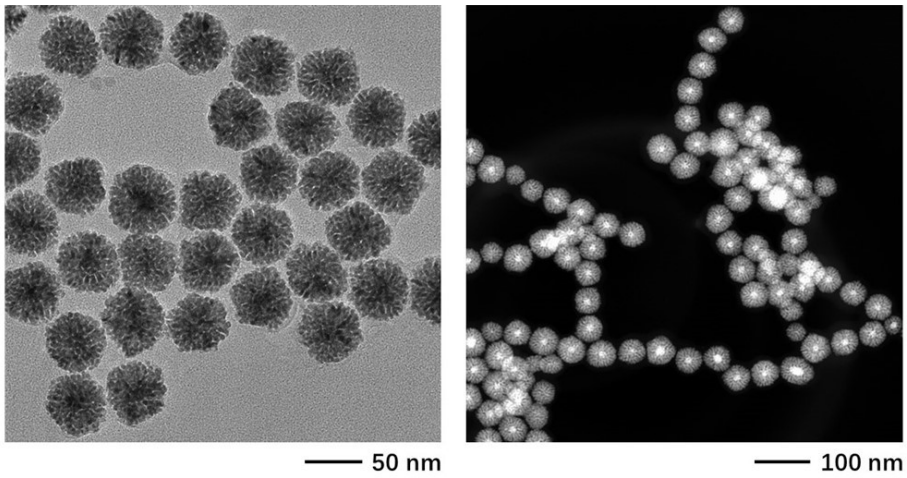

Fig. S2. The representative bright-field and dark-field TEM images of Au@Pd core-porous shell NPs.

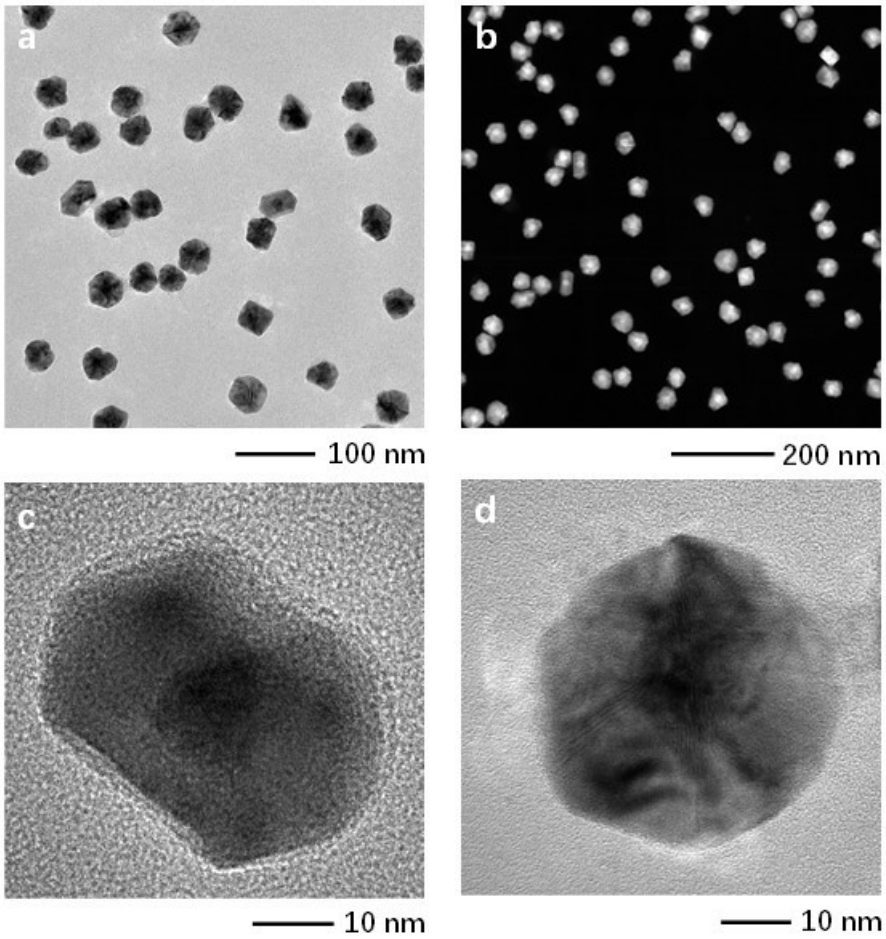

Fig. S3. (a) Bright-field, (b) dark-field, and (c, d) high-resolution TEM images of Au@Pd core-shell NPs synthesized in the presence of CTAB.

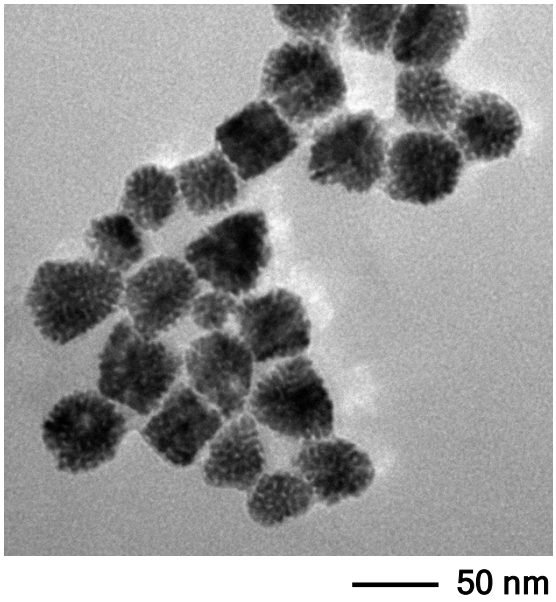

Fig. S4. TEM image of porous Pd NPs synthesized in the absence of Au seeds.

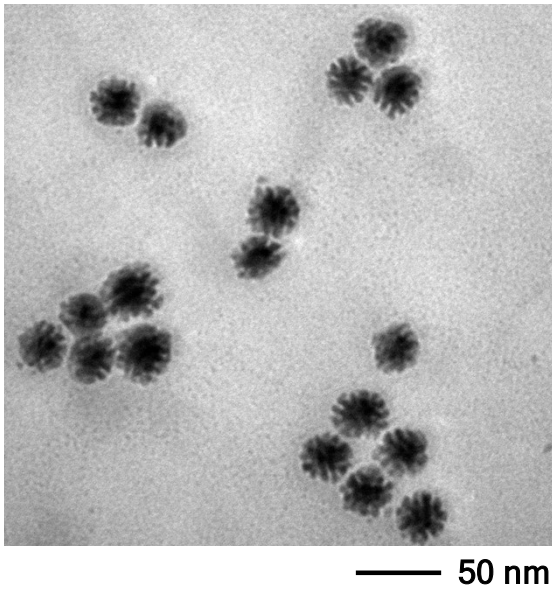

Fig. S5. TEM image of Au@Pd core-shell NPs synthesized using HDPC instead of using CTAC.

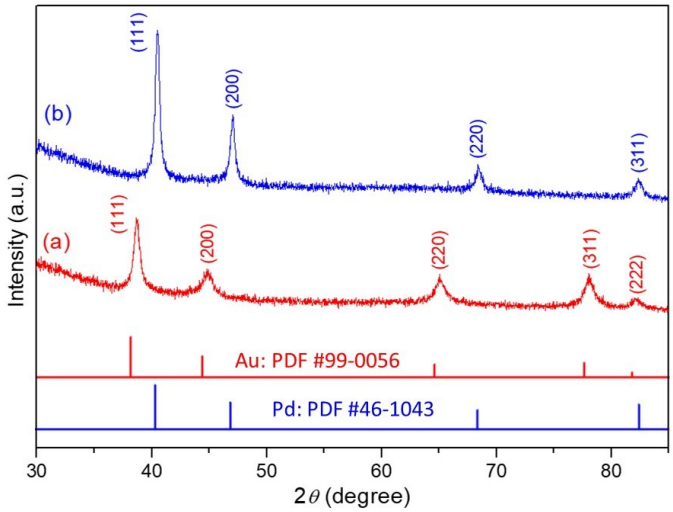

Fig. S6. XRD patterns of (a) Au seeds and (b) Pd NPs.

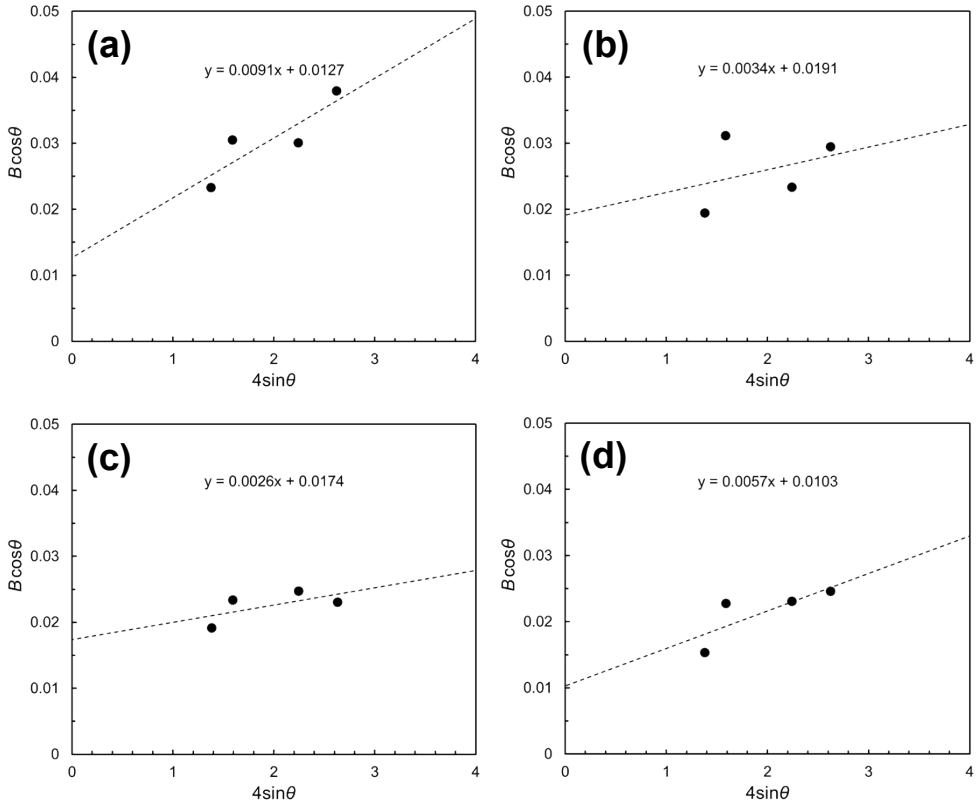

Fig. S7. Williamson-Hall analysis of the strain of Pd shell in Au@Pd core-porous shell NPs with different sizes: (a) 23.7 nm, (b) 35.2 nm, (c) 44.2 nm, and (d) 57.5 nm.

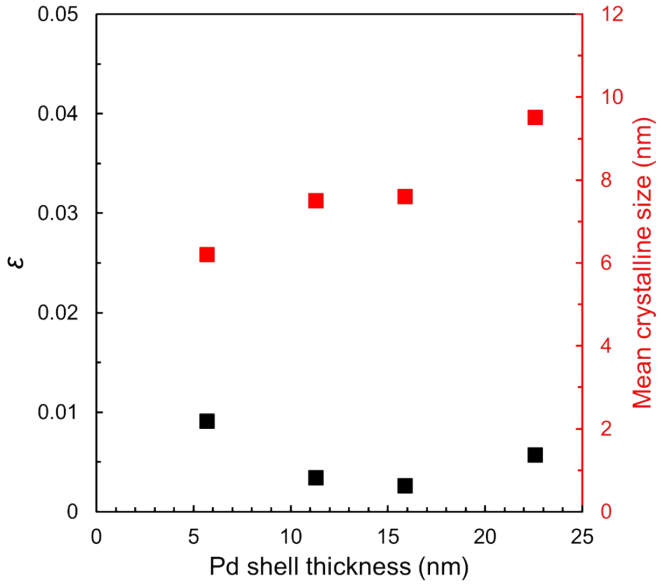

Fig. S8. The relation of Pd shell thickness in Au@Pd core-porous shell NPs with strain (ε) and mean crystalline size of Pd calculated by the Scherrer formula using the (111) peak of Pd.

Table S1. Peak parameters obtained by deconvolution of Pd 3d peaks.

			23.7 nm	35.2 nm	44.2 nm	57.5 nm
Pd shell thickness (nm)			5.7	11.3	15.9	22.6
Pd^0	$3d_{5/2}$	Peak position (eV)	335.0	335.2	335.2	335.2
		FWHM (eV)	1.51	1.50	1.36	1.31
	$3d_{3/2}$	Peak position (eV)	340.2	340.5	340.5	340.5
		FWHM (eV)	1.36	1.56	1.39	1.34
	Spin-orbit intensity ratio		1.49	1.49	1.53	1.49
Pd^{2+} (PdO)	$3d_{5/2}$	Peak position (eV)	336.1	336.1	336.1	336.1
		FWHM (eV)	1.64	2.5	2.5	2.5
	$3d_{3/2}$	Peak position (eV)	341.4	341.4	341.4	341.4
		FWHM (eV)	1.18	2.5	2.5	2.5
	Spin-orbit intensity ratio		1.49	1.49	1.49	1.49
Pd^{4+} (PdO_2)	$3d_{5/2}$	Peak position (eV)	337.6	338.0	338.0	338.0
		FWHM (eV)	1.60	1.64	1.93	1.79
	$3d_{3/2}$	Peak position (eV)	342.9	343.3	343.3	343.3
		FWHM (eV)	1.61	1.68	1.82	1.81
	Spin-orbit intensity ratio		1.49	1.49	1.49	1.49

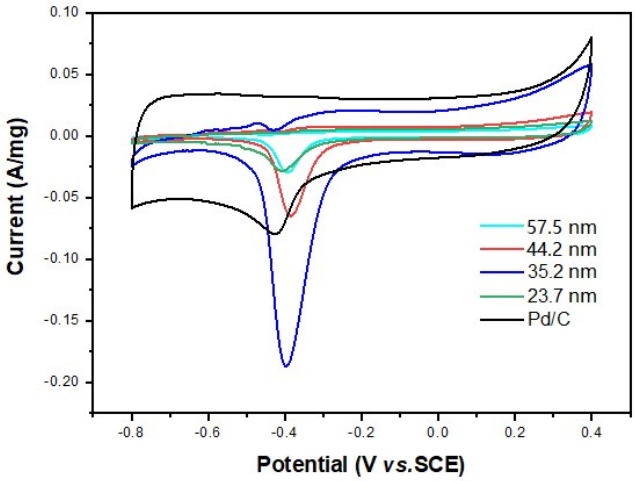

Fig. S9. CV curves of the Au@Pd/PdO_x core-porous shell NPs with different sizes and commercial Pd/C in 1 M KOH solution.

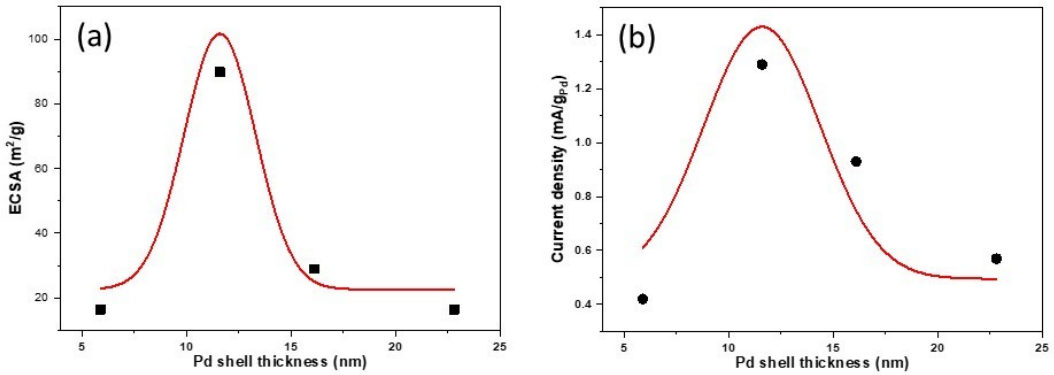

Fig. S10. (a) The ECSAs and (b) current density of Au@Pd/PdO_x core-porous shell NPs to ethanol electrooxidation versus the Pd shell thickness.